Complexation of NpO2+ with Amine-Functionalized Diacetamide Ligands in Aqueous Solution: Thermodynamic, Structural, and Computational Studies

Complexation of NpO_2^+ with Amine-Functionalized Diacetamide Ligands in Aqueous Solution: Thermodynamic, Structural, and Computational Studies

Yang Gao,[a,b] Phuong V. Dau,[a] Bernard F. Parker,[a,c] John Arnold,[a,c] Andrea Melchior,[d,*] Zhicheng Zhang,[a,*] Linfeng Rao[a]

[a]Chemical Sciences Division, Lawrence Berkeley National Laboratory, 1 Cyclotron Road, Berkeley, California 94720, USA.

[b]College of Nuclear Science and Technology, Harbin Engineering University, Harbin, China

[c]Department of Chemistry, University of California – Berkeley, Berkeley, CA 94720, USA

[d]Dipartimento Politecnico di Ingegneria e Architettura, Università di Udine, Laboratori di Chimica, via delle Scienze 99, 33100 Udine, Italy

Abstract

Complexation of Np(V) with three structurally-related amine-functionalized diacetamide ligands, including 2,2'-(benzylazanediyl)bis(N,N'-dimethylacetamide) (BnABDMA), 2,2'-azanediylbis(N,N'-dimethylacetamide) (ABDMA), and 2,2'-(methylazanediyl)bis(N,N'-dimethylacetamide) (MABDMA), in aqueous solutions was investigated. The stability constants of two successive complexes, NpO_2L^+ and $NpO_2L_2^+$ where L stands for the ligands, were determined by absorption spectrophotometry. The results suggest that the stability constants of corresponding Np(V) complexes follow the trend: MABDMA > ABDMA ≈ BnABDMA. The data are discussed in terms of the basicity of the ligands and compared with those for the complexation of Np(V) with an ether oxygen-linked diacetamide ligand. EXAFS data indicate that, similar to the complexation with Nd^{3+} and UO_2^{2+}, the ligands coordinate to NpO_2^+ in a tridentate mode through the amine nitrogen and two oxygen atoms of the amide groups. Computational results, in conjunction with spectrophotometric data, verified that the 1:2 complexes ($NpO_2(L)_2^+$) in aqueous solutions are highly symmetric with Np at the inversion center,

so that the *f-f* transition of NP(V) is forbidden and $NpO_2(L)_2^+$ does not display significant absorption in the near-IR region.

Key Words: Neptunium, Diacetamide, Complexation, Thermodynamics, Symmetry

1. Introduction

Neptunium is considered to be a problematic element in the spent nuclear fuel (SNF) reprocessing as well as in the environmental management of nuclear wastes due to its chemical behavior and transport characteristics in the geological environment. Among the radionuclides in SNF and high-level nuclear wastes (HLW), ^{237}Np is one of the most soluble and is most likely to migrate away from the HLW repository. Owing to its long half-life, $t_{1/2} = 2.144 \times 10^6$ years, ^{237}Np is predicted to become a major radiological hazard, contributing 67% of the total radiation dose from HLW after 75000 years.[1] The pentavalent state of neptunium, Np(V), is the most stable state and exists as NpO_2^+ ions in aqueous solution. Because of its low ionic charge and relatively large ionic radius, NpO_2^+ ion does not form strong complexes with many ligands and is difficult to be extracted by many traditional extractants in actinide separation processes. Also, NpO_2^+ is highly mobile in the geological environment because of its weak tendencies toward hydrolysis, precipitation, or sorption by the geomedia. It is of prime importance to find ligands that can strongly bind $NpO_2^+$and separate it from HLW so that the nuclear waste can be safely disposed of in geological repositories.

Numerous studies have been conducted to understand the complexation of neptunium with organic ligands including monocarboxylic acids such as benzoic acid[2] and picolinic acid,[3] dicarboxylic acids such as dipicolinic acid (H_2DPA),[4] 1,10-phenanthroline-2,9-dicarboxylic acid ($H_2PhenDA$),[5] iminodiacetic acid (IDA)[6,7] and N-methyl-iminodiacetic acid (MIDA),[8,9] and

glutaroimide-dioxime.[10] These ligands exhibit fairly good complexation capabilities with Np(V) and have the potential to be used as efficient complexants for neptunium. In addition, these ligands are all composed of only C, H, O, and N atoms, so that they are completely combustible and the volume of solid wastes generated in the separation processes could be significantly reduced.

In recent years, alkyl-substituted diglycolamides have been studied as efficient complexants for separations of actinides and lanthanides in SNF reprocessing.[10] Diglycolamides contain ether oxygen linkage between two amide groups and usually form tridentate complexes with metal ions using the three oxygen donor atoms from the ether and the two amide groups. These ligands also contain only C, H, O, and N atoms and their use helps to make the separation processes more environmentally sustainable. Besides, by varying the substitution groups on the amide nitrogen, the diglycolamides can be used either as efficient extractants in solvent extraction such as N,N,N',N'-tetraoctyl- diglycolamide (TODGA)[11] and N,N,N',N'-tetraisobutyl- diglycolamide (TiBDGA),[12] or as small molecules for single-phase thermodynamic studies such as N,N,N',N'-tetramethyl-diglycolamide (TMDGA).[13]

Replacing the ether oxygen linkage in diglycolamides with amine linkage, we have synthesized a series of diacetamide ligands, including 2,2'-(benzylazanediyl)bis(N,N'-dimethylacetamide) (BnABDMA), 2,2'-azanediylbis(N,N'-dimethylacetamide) (ABDMA), and 2,2'-(methylazanediyl)bis(N,N'-dimethylacetamide) (MABDMA) (Figure 1), and determined the thermodynamic parameters of the complexation of these ligands with Nd(III)[14] and U(VI).[15] The amine nitrogen linkage in these ligands allows fine-tuning of the ligand basicity and binding strength with metal ions via substitution on the central amine N atom with different functional groups, which is not feasible for the ligands with the ether-linkage such as TMDGA. The data for the complexation with Nd(III)[14]and U(VI)[15] show that the stability of the complexes

follow the trend: MABDMA > ABDMA > BnABDMA, agreeing with the order of the basicity of the nitrogen donor atom in these ligands. It is the focus of the present study to extend the thermodynamic studies to NpO_2^+ and compare the data with those for Nd^{3+} and UO_2^{2+}.

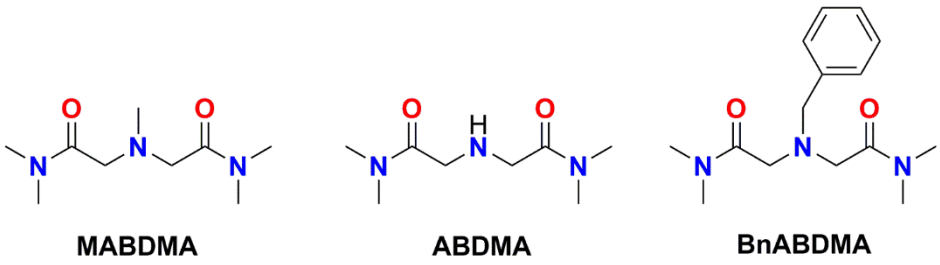

Figure 1 Structures of MABDMA, ABDMA, and BnABDMA.

One interesting feature of the complexation of NpO_2^+ with the ether oxygen linked diacetamide ligand, TMDGA, is that the 1:2 complex, $NpO_2(L)_2^+$ where L = TMDGA, is "silent" in near-IR absorption spectroscopy,[12] which is interpreted as the presence of an inversion center where the Np atom locates that makes the f-f transition forbidden by the Laporte's rule.[16] The "silent" feature in absorption spectroscopy of NpO_2^+ has also been theoretically discussed in the literature.[17–20] In the case of the $NpO_2(L)_2^+$ complex with the amine-functionalized diacetamides (where L = BnABDMA, ABDMA, or MABDMA), the two ligands could be in *cis*- or *trans*-configuration with respect to the equatorial plane of NpO_2^+, resulting in the absence or presence of an inversion center. Therefore, it is fundamentally interesting to determine, in addition to thermodynamic data, the optical absorption properties of the complexes and correlate these with the symmetry of the complexes.

In this work, the stability constants of the NpO_2^+ complexes with BnABDMA, ABDMA, and MABDMA were determined by spectrophotometry. The data are compared with those of Nd^{3+} and

UO_2^{2+} in the literature. EXAFS and computational studies were conducted to help interpret the data and correlate the optical properties with the symmetry of the NpO_2^+ complexes.

2. Experimental

2.1 Chemicals

All chemicals are reagent grade or higher. 2,2'-(benzylazanediyl)bis(N,N'-dimethylacetamide) (BnABDMA), 2,2'-azanediylbis(N,N'-dimethylacetamide) (ABDMA), and 2,2'-(methylazanediyl)bis(N,N'-dimethylacetamide) (MABDMA) were synthesized according to previous procedures.[14] Details of the preparation and characterization are provided in the literature.[14] The starting materials and solvents used in the preparation were purchased from commercial suppliers (Sigma-Aldrich, Alfa Aesar, EMD, and TCI) and used without further purification.

Boiled Milli-Q water was used in the preparation of all solutions. All experiments were conducted at 25 ºC and an ionic strength of 1.0 M $NaNO_3$. The ionic medium of $NaNO_3$, instead of $NaClO_4$, was chosen for this work because the solubility of the metal complexes with the diacetamide ligands is low in $NaClO_4$ solutions. The stock solution of Np(V) was prepared as described elsewhere.[21] The concentration of Np(V) was determined by the absorbance at 980.2 nm (ε = 395 M^{-1} cm^{-1}), and the concentration of free acid in the stock solution was determined by Gran's titration.[22] Stock solutions of the three ligands were prepared by dissolving appropriate amounts of the ligands in 1.0 M $NaNO_3$. The concentration of the ligands was directly calculated from the weight and verified by potentiometric titrations.

2.2 Spectrophotometry

Spectrophotometric titrations were carried out to confirm the stability constants of the NpO_2^+ complexes with ligands using a Cary 6000i UV-Vis-NIR spectrophotometer (Varian Inc.) with a 10 mm cuvette (1 nm spectral bandwidth). The temperature of the sample was maintained at (25.0 ± 0.1) ^oC by a constant-temperature controller associated with the instrument. Absorption spectra were collected from 1065 nm to 950 nm with a 0.2 nm step. For a typical titration experiment, appropriate aliquots of ligand solution were added into a cuvette containing 2.1 mL of NpO_2^+ solution. The solution in the cuvette was mixed thoroughly for 1-2 minutes before the spectrum was collected. Prior studies have shown that the complexation reaction was fast and the absorbance became stable within 30 seconds of mixing. Usually, 20 or more additions were made, generating a set of 21 or more spectra in each titration. Multiple titrations with different concentrations of Np(V) were performed. The formation constants were calculated by nonlinear least-squares regression analysis using the commercially available HypSpec program.[23]

In this paper, the neutral ligands, protonated ligands, and the NpO_2^+ complexes are denoted as L, HL^+, and $NpO_2(L)_j^+$, respectively, where j = 1, and 2.

2.3 EXAFS

Six Np(V) solution samples were prepared for EXAFS study at Stanford Synchrotron Radiation Laboratory. Solution I does not contain the ligands and represents the free NpO_2^+ ion. Solutions II and III contain Np(V) and MABDMA in different concentrations so that $NpO_2(MABDMA)^+$ and $NpO_2(MABDMA)_2^+$ are the dominant complexes in Solution II and III, respectively. Solutions IV and V contain Np(V) and ABDMA in different concentrations so that $NpO_2(ABDMA)^+$ and $NpO_2(ABDMA)_2^+$ are the dominant complexes in Solution IV and V, respectively. Solution VI

contains Np(V) and BnABDMA and the dominant complex is $NpO_2(BnABDMA)_2^+$. The solution samples (each 2.0 mL) were contained in plastic vials and sealed in plastic bags. The samples were mounted on a sample positioner with Scotch tape, and measured on Beamline 11- 2. Neptunium L_{III}-edge data were collected up to k_{max} ~ 14 $Å^{-1}$ in both transmission and fluorescence modes. Multiple scans (3-4) were taken for each sample.

Energy-calibration was conducted by assigning the first inflection point of the K edge of yttrium (Y foil as the reference) at 17,038 eV. Data reduction, including pre-edge background subtraction followed by spline fitting and normalization, was performed with the program Athena.[24] The EXAFS data were extracted above the threshold energy, E_0, defined as 17,166 eV. The fit of EXAFS data utilized the theoretical phases and amplitudes calculated by the program FEFF7[25] starting with the model crystal structure of a 1:2 U(VI) complex $UO_2L_2(ClO_4)_2$ where L denotes 2,2'-(trifluoroazanediyl)bis(N,N'-dimethylacetamide) (CCDC 1584249) and elongating the U-N and U-O bonds in this structure for corresponding Np-N and Np-O bonds. For each sample, selected single scattering (SS) and multiple scattering (MS) paths from the FEFF calculation were used in the fit based on the proposed coordination mode. In all the fits, an amplitude factor (S_0^2) and a threshold energy shift (ΔE_0) were considered to be global parameters. Hanning windows with a k range (3.0 - 14.0 $Å^{-1}$) and Fourier transform with an R range (0.95 – 3.5 Å) were used. The fit factor (r) is provided as an indication of the fit quality.

2.4 Computation

Density functional theory (DFT) calculations were carried out on the complexes and ligands using the three-parameter hybrid functional B3LYP.[26,27] This level of theory has previously been demonstrated to generate reliable structural and energetic results for actinide complexes.[15,28,29]

Grimme's D3 empirical dispersion correction[30] has also been employed as it has been demonstrated to be important when calculating the binding energies of ligands of different bulkiness.[31] Stuttgart-Dresden small-core quasi-relativistic effective core potentials have been employed for neptunium.[32] Other elements were treated using a 6-31++G(d,p) Gaussian-type basis set. Solvent effect has been taken into account by using the polarizable continuum model (PCM).[33] Geometry optimizations of the $NpO_2(L)_2^+$ complexes were run with symmetry constraints in PCM solvent (the point groups are reported with the optimized structures in the section of results). The free energies of the complexes were calculated by adding to the electronic energy of each complex the zero point energy and thermal corrections, which comprise electronic, vibrational, rotational, and translational contributions to the internal energy. All calculations were carried out using the Gaussian16 program.[34]

3. Results and Discussion

3.1 Stability constants of Np(V) complexes with BnABDMA, ABDMA, and MABDMA

A representative set of absorption spectra for the titration of Np(V) with MABDMA is shown in Figure 2. In this titration, a solution of Np(V) in the cuvette was titrated with a solution of the ligand. The variations of spectra during the titration can be described in two phases: (1) Phase I (cyan color) where the intensity of the absorption band of free NpO_2^+ around 980 nm decreased and a new band appears at 988 nm and intensified as the concentration of ligand increases， indicating the formation of a Np(V) complex (probably a 1:1 complex); and (2) Phase II (rose color) where the intensity at 988 nm decreased but no new absorption peaks appeared at longer wavelengths.

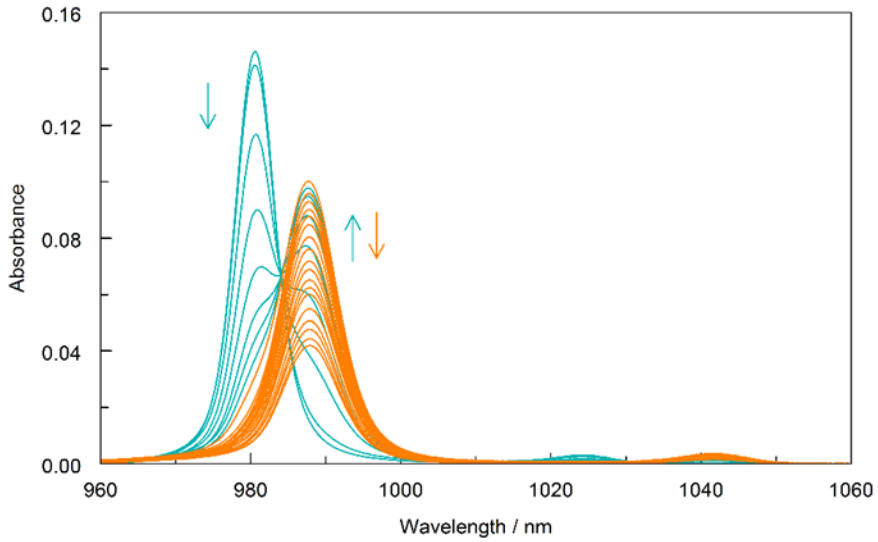

Figure 2 Spectrophotometric titration of NpO_2^+ complexation with MABDMA (I = 1.0 M $NaNO_3$, t = 25°C). Initial concentrations in cuvette: C_{Np} = 0.386 mM, C_H = 0.443 mM, $C_{nitrate}$ = 1.00 M; titrant: C_L = 38.0 mM, $C_{nitrate}$ = 1.00 M. The variations of the spectra during the titration are discussed in two phases: Phase I (cyan color) and Phase II (rose color).

These observations, different from those for Np(V) complexes with many ligands (e.g., oxalate, fluoride, sulfate, picolinate, glutaroimide-dioxime) where the decrease of the absorbance of the first complex is accompanied by the appearance of new absorption band(s) of successive complexes at longer wavelengths,[3,10,35,36,37] are very similar to those for the ligands that form centrosymmetric 1:2 Np(V) complexes (e.g., DPA, TMDGA, MIDA, ODA).[4,9,13,38,39]

Accordingly, the spectrophotometric titration data could be interpreted as showing the successive formation of the 1:1 and 1:2 Np(V)/L complexes (reactions 1 and 2), with the 1:1 complex absorbing at 988 nm and the 1:2 complex does not absorb in the experimental wavelength region. This interpretation is consistent with the spectra factor analysis that suggests, besides the free NpO_2^+ and $NpO_2(NO_3)_{(aq)}$ complex, there is only one additional absorbing species, i.e., presumably, the 1:1 $NpO_2(L)^+$ complex in the solutions.

$$NpO_2^+ + L = [NpO_2L]^+ \quad (1)$$

$$NpO_2L^+ + L = [NpO_2L_2]^+ \quad (2)$$

The variations of spectra in the spectrophotometric titrations with all three ligands are similar and shown in Figure 3. The first row of Figure 3 represents Phase I of the titrations where the formation of $NpO_2(L)^+$ is dominant (reaction (1)), while the second row represents Phase II of the titrations where the formation of $NpO_2(L)_2^+$ is dominant (reaction (2)). The third row shows the calculated molar absorptivities of the $NpO_2(L)^+$ complexes.

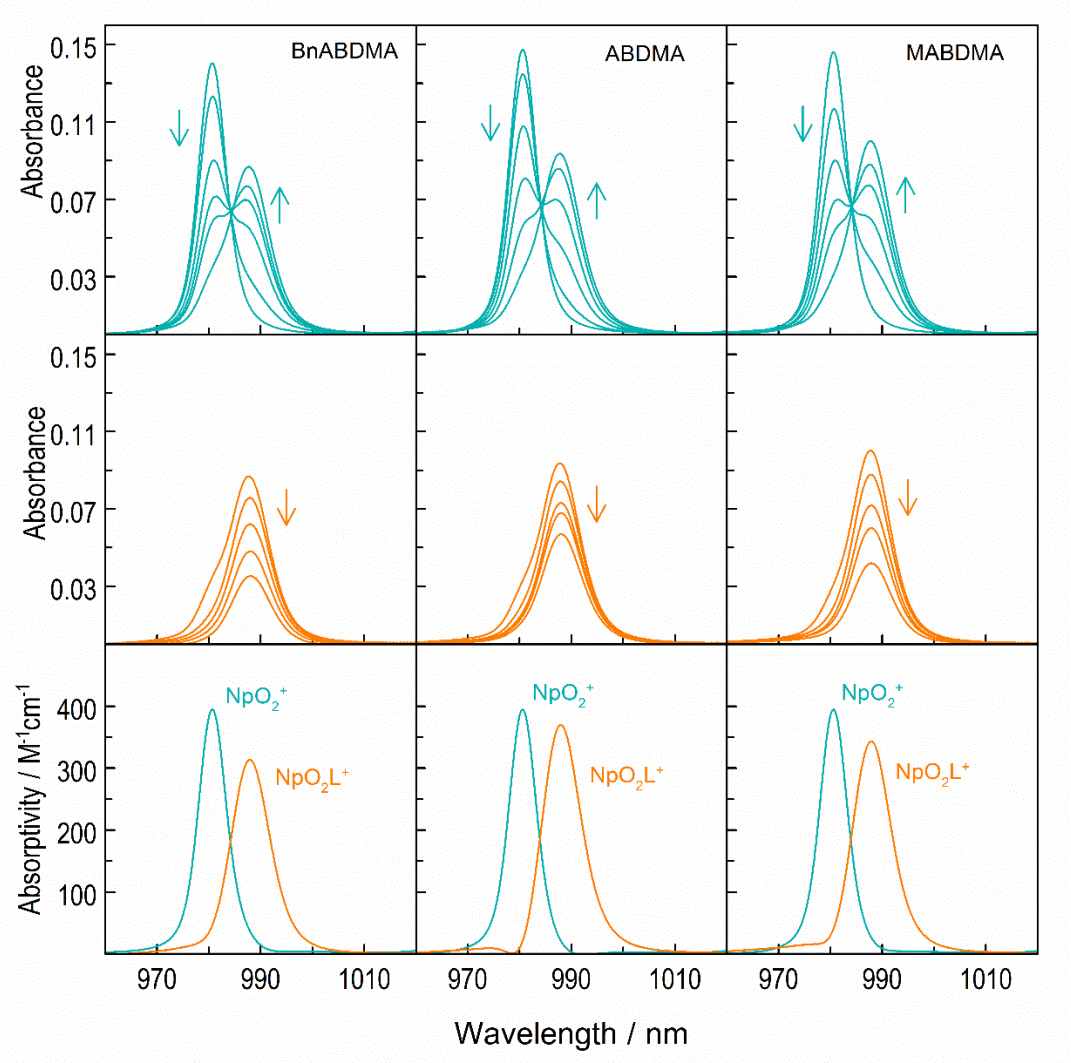

Figure 3 Analysis of spectrophotometric titration data for the complexation of NpO_2^+ with BnABDMA, ABDMA, and MABDMA. The first row: Phase I of the titration showing the decrease of free NpO_2^+ and the formation of $NpO_2(L)^+$; the second row: Phase II of the titration showing the decrease of $NpO_2(L)^+$ with no new absorption bands for the formation of $NpO_2(L)_2^+$; the third row: molar absorptivities of NpO_2^+ and $NpO_2(L)^+$; the molar absorptivity of NpO_2NO_3 is omitted for clarity.

Best fit of the spectra was obtained by fitting the data with the model including the formation of two successive NpO_2^+ complexes as shown by reactions (1) and (2) and the calculated equilibrium constants are shown in Table 1, in comparison with the constants for the complexation of NpO_2^+ with TMDGA from the literature.[13]

Table 1 Equilibrium constants for the protonation and complexation of BnABDMA, ABDMA, and MABDMA, with NpO_2^+ at 25 ºC and I = 1.0 M $NaNO_3$.

Ligand	Reaction	Method[a]	logβ	Ref.
BnABDMA	$H^+ + L = HL^+$	pot, cal	6.36 ± 0.09	14
	$NpO_2^+ + L = NpO_2(L)^+$	sp,	2.90 ± 0.09	p.w.
	$NpO_2^+ + 2L = NpO_2(L)_2^+$	sp,	4.01 ± 0.09	
ABDMA	$H^+ + L = HL^+$	pot, cal	7.12 ± 0.09	14
	$NpO_2^+ + L = NpO_2(L)^+$	sp,	2.80 ± 0.09	p.w.
	$NpO_2^+ + 2L = NpO_2(L)_2^+$	sp,	4.00 ± 0.09	
MABDMA	$H^+ + L = HL^+$	pot, cal	7.64 ± 0.09	14
	$NpO_2^+ + L = NpO_2(L)^+$	sp,	3.59 ± 0.09	p.w.
	$NpO_2^+ + 2L = NpO_2(L)_2^+$	sp,	5.50 ± 0.09	
TMDGA	$NpO_2^+ + L = NpO_2(L)^+$	Sp	1.37 ± 0.01	13
	$NpO_2^+ + 2L = NpO_2(L)_2^+$	Sp	2.47 ± 0.01	

3.2 Comparison of the binding strength among the three amine-functionalized diacetamides

For both $NpO_2(L)^+$ and $NpO_2(L)_2^+$ complexes, the binding strength of the three ligands follows the order: MABDMA > ABDMA ≈ BnABDMA. This order is in fair agreement with those observed for the complexation with Nd(III)[14] and U(VI),[15] where MABDMA > ABDMA > BnABDMA. These trends are interpreted as reflecting the complexation reactions are predominantly electrostatic interactions: the electron-donating methyl group increases and the electron-withdrawing benzyl group decreases the electron density on the amine nitrogen, resulting in stronger metal complexes with MABDMA than those with BnABDMA and ABDMA.

3.3 Comparison of the binding strength between the amine-linked ligands and ether oxygen-linked TMDGA

As shown in Table 1, all three amine-linked ligands form stronger complexes with NpO_2^+ than the ether oxygen-linked TMDGA. Such trend is often observed when comparing the binding strength between nitrogen-donor and oxygen donor ligands in aqueous solution. For example, metal complexes with iminodiacetic acid (IDA) are stronger than those with oxydiacetic acid (ODA).[40] The difference in binding is usually attributed to the higher basicity and less hydration of amine/imine nitrogen than ether oxygen in aqueous solutions, supported by the difference in the enthalpy and entropy of complexation between the two groups of ligands in the complexation of metal ions.

3.4 Identification of Np(V) complexes in solution by EXAFS

The k^3-weighted EXFAS spectra and the FT magnitude of the six neptunium solution samples are shown in Figure 4. The fitting results are shown in Table 2.

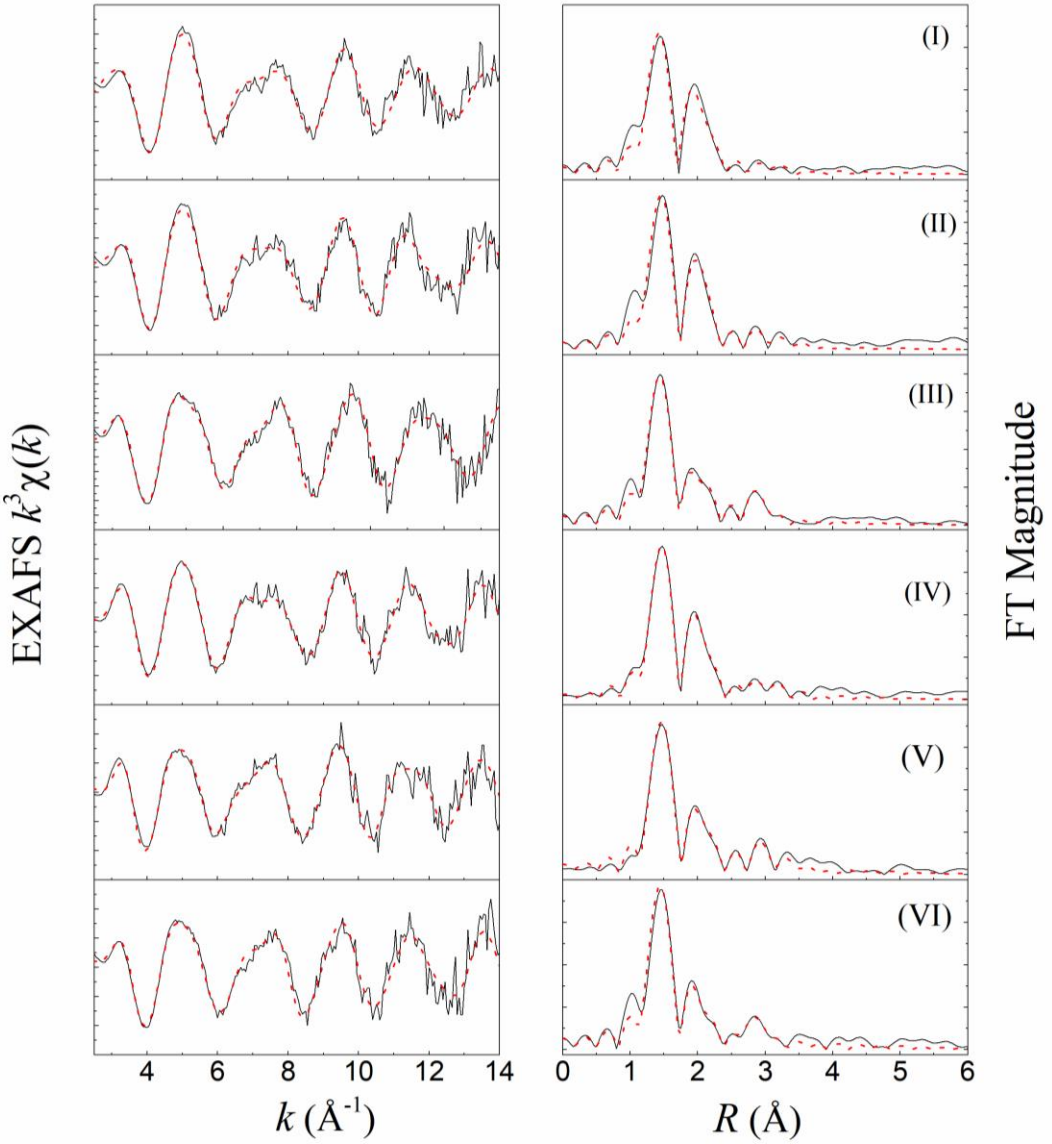

Figure 4 EXAFS spectra (left) and FT magnitude (right).

Table 2 shows the experimentally observed structure parameters for the Np species in six solution samples. For the free NpO_2^+ ion (Solution I), five oxygen atoms (from water molecules) were identified in the equatorial plane, consistent with observation in the literature.[41,42] For the solutions where the $NpO_2(L)^+$ complexes are dominant (solutions II and IV), one nitrogen atom

and four oxygen atoms in the equatorial plane were observed, suggesting there is one ligand and two water molecules coordinating to Np and the ligand is tridentate using the amine nitrogen and two oxygen atoms from the amide groups. For the solutions where the $NpO_2(L)_2^+$ complexes are dominant (solutions III, V, and VI), two nitrogen atoms and four oxygen atoms in the equatorial plane were observed, suggesting there are two ligand molecules coordinating to Np and, same as in the $NpO_2(L)^+$ complexes, the ligand is tridentate using the amine nitrogen and two oxygen atoms from the amide groups.

The EXAFS data provide evidence that, despite its "silent" feature in the absorption spectra, the 1:2 complexes, $NpO_2(L)_2^+$, are in fact present in solutions where the ligand/metal ratio is high.

Table 2 EXAFS fitting results of Np(V) species in solutions

Solution[a]	Shell	N[b]	R (Å)	σ^2	Notice
I (Free Np(V))	Np-O_{ax}	2.0	1.82 ± 0.01	0.0025	S_0^2 = 1.0, ΔE^0 = 9.5 eV
100 % NpO_2^+	Np-O_{eq}	4.9 ± 1.1	2.46 ± 0.02	0.0043	r = 0.0017
II (Np(V)/MABDMA)	Np-O_{ax}	2.0	1.82 ± 0.01	0.0019	S_0^2 = 1.0, ΔE^0 = 8.4 eV
15 % NpO_2^+	Np-O_{eq}	4.1 ± 1.0	2.45 ± 0.04	0.0042	r = 0.0067
75 % $NpO_2(L)^+$					
10 % $NpO_2(L)_2^+$	Np-N_{eq}	1.0 ± 0.2	3.02 ± 0.13	0.0036	
III (Np(V)/MABDMA)	Np-O_{ax}	2.0	1.82 ± 0.01	0.0018	S_0^2 = 1.0, ΔE^0 = 8.9 eV
10 % $NpO_2(L)^+$	Np-O_{eq}	3.9 ± 1.0	2.49 ± 0.04	0.0051	r = 0.0030
90 % $NpO_2(L)_2^+$	Np-N_{eq}	2.0 ± 0.4	3.05 ± 0.10	0.0041	
IV (Np(V)/ABDMA)	Np-O_{ax}	2.0	1.81 ± 0.01	0.0017	S_0^2 = 0.86, ΔE^0 = 8.8 eV
10 % NpO_2^+	Np-O_{eq}	4.3 ± 1.1	2.45 ± 0.02	0.0086	r = 0.0021
75 % $NpO_2(L)^+$					
15 % $NpO_2(L)_2^+$	Np-N_{eq}	1.1 ± 0.2	3.11 ± 0.10	0.0027	
V (Np(V)/ABDMA)	Np-O_{ax}	2.0	1.82 ± 0.02	0.0019	S_0^2 = 0.93, ΔE^0 = 8.9 eV
10 % $NpO_2(L)^+$	Np-O_{eq}	4.1 ± 0.8	2.48 ± 0.05	0.0049	r = 0.0055
90 % $NpO_2(L)_2^+$	Np-N_{eq}	1.9 ± 0.4	3.10 ± 0.09	0.0035	
VI (Np(V)/BnABDMA)	Np-O_{ax}	2.0	1.82 ± 0.02	0.0017	S_0^2 = 1.0, ΔE^0 = 8.9 eV
5 % $NpO_2(L)^+$	Np-O_{eq}	3.9 ± 0.8	2.47± 0.06	0.0052	r = 0.043
95% $NpO_2(L)_2^+$	Np-N_{eq}	1.9 ± 0.4	3.07 ± 0.11	0.0045	

[a] The Np(V) speciation (relevant to total [Np]) was calculated by using the complexation constants which were determined in this work.

[b] N = 2.0 held constant for Np-O_{ax} path in the fit of every solution.

3.5 Symmetry and optical absorption: computational data

Minimum energy structures of each $NpO_2L_2^+$ complex (L = ABNMA, MABDMA, and BnABDMA) were obtained for three types of isomers as shown in three columns of Figure 5. Two types of centrosymmetric isomers are represented, respectively, in the first column (A, D, and G) and in the second column (B, E, and H). These two types of isomers were previously shown to be present in similar U(VI) systems.[15] The third type of isomers are non-centrosymmetric and shown in the third column of Figure 5 (C, F, and I).

$NpO_2(ABDMA)_2^+$	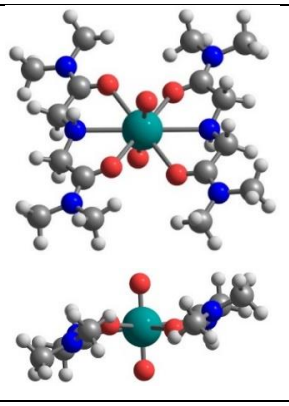	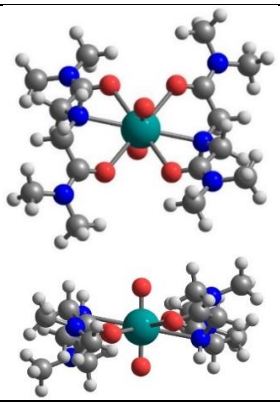	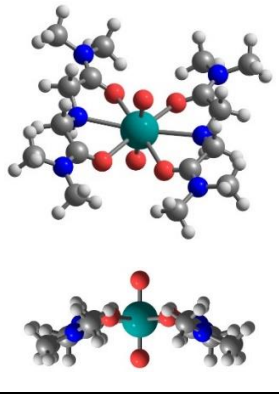
	A (C_{2h})	B (C_{2h})	C (C_s)
$NpO_2(MABDMA)_2^+$	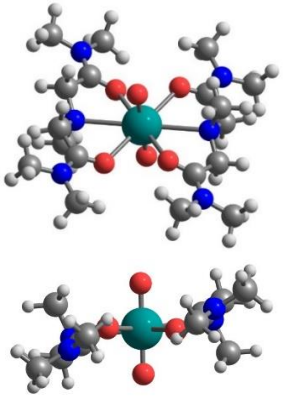	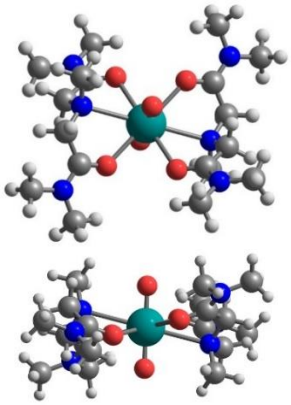	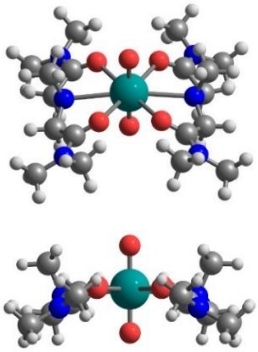
	D (C_{2h})	E (C_{2h})	F (C_s)
$NpO_2(BnABDMA)_2^+$	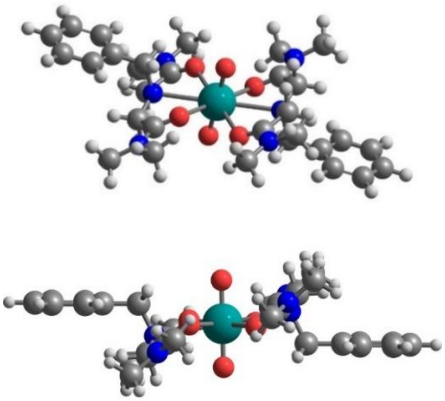	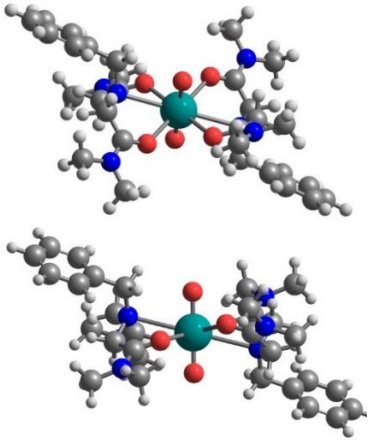	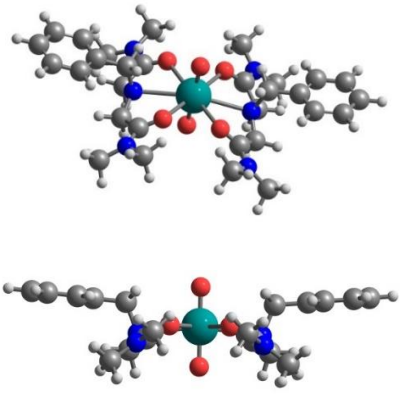
	G (C_{2h})	H (C_{2h})	I (C_s)

Figure 5. Calculated minimum energy structures and the molecular point groups of the $NpO_2(L)_2^+$ complexes. For each complex, the upper row represents the structures viewed from the top of the equatorial plane of NpO_2^+, and the lower row represents the structures viewed along the equatorial plane of NpO_2^+.

The structures in the first and the second columns of Figure 5 are centrosymmetric (C_{2h} point group) with the Np atom at the inversion center, but they differ in the arrangements of the " >-C-N-C-N< " backbone with respect to the equatorial plane of NpO_2^+. The diacetamide ligands are nearly planar (the O-C··C-O dihedral angle ~ 0°), in a in the A, D, G structures, while non-planar in B, E, H (O-C··C-O dihedral angle ~ 30°). In Table S2 the values for relevant bond lengths are reported. The calculated axial Np-O bond is accurately reproduced in all cases. The Np-N lengths are systematically underestimated with respect to EXAFS data, while the and Np-O_{eq} are overestimated. This trend was also observed for the similar complexes with UO_2^{2+}, although calculations were carried out with a different functional (B3LYP).

Calculations indicate that the structures in the first column (A, D, and G) always possess lower energies than those in the second column (B, E, and H) in aqueous media (Table S2). Therefore, the following discussion on the comparison of energy between the centrosymmetric and non-centrosymmetric complexes is focused on the structures in the first column (centrosymmetric A, D, and G) and the third column (non-centrosymmetric C, F, and I).

The energies of the non-centrosymmetric structures relative to those of the centrosymmetric structures were calculated and shown in Table 3. For the 1:2 complexes of NpO_2^+ with ABNMA, MABDMA, and BnABDMA, the non-centrosymmetric structures (C, F, and I) possess energies higher than the centrosymmetric structures (A, D, and G) by 5.2, 8.4, and 22.2 $kJ \cdot mol^{-1}$, respectively. This means that the $NpO_2(L)_2^+$ complexes in aqueous solution are most likely to be centrosymmetric.

Table 3 Relative free energy ΔG of the structures of $NpO_2(L)_2^+$ complexes in aqueous solution.

Complex		Structure	ΔG_{water}, kJ·mol^{-1}
$NpO_2(ABDMA)_2^+$	A (C_{2h})	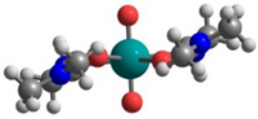	0.0
	C (C_s)	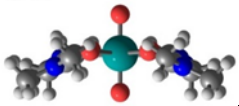	8.4
$NpO_2(MABDMA)_2^+$	D (C_{2h})	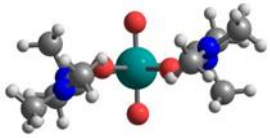	0.0
	F (C_s)	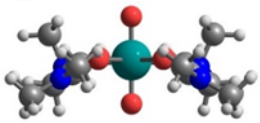	5.2
$NpO_2(BnABDMA)_2^+$	G (C_{2h})	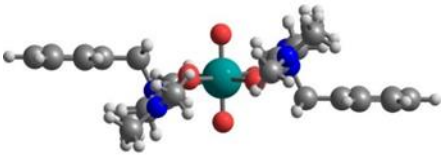	0.0
	I (C_s)	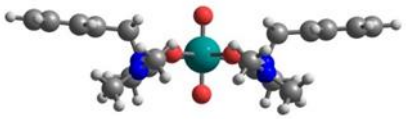	22.2

It is known that the near IR absorption bands of NpO_2^+ originate from the f-f transitions that are electric-dipole forbidden by Laporte's rule. A number of studies on NpO_2^+ complexes have demonstrated that, if the Np(V) complex is centrosymmetric and the neptunium atom is at the inversion center, the *f-f* transitions of Np(V) are completely forbidden and the near-IR absorption bands will be "silent".[38,43,44] Only if the arrangement of ligands around NpO_2^+ destroys the inversion center, absorption bands of Np(V) are observed. Integrating the experimental data from spectrophotometric titrations, the structural data from EXAFS, and the theoretical DFT calculated results in this work, the optical absorption properties and schematic structures of the Np(V) species (free aquo NpO_2^+ ion, $NpO_2(L)^+$, and $NpO_2(L)_2^+$ where L = MABDMA) can be described in Figure 6.

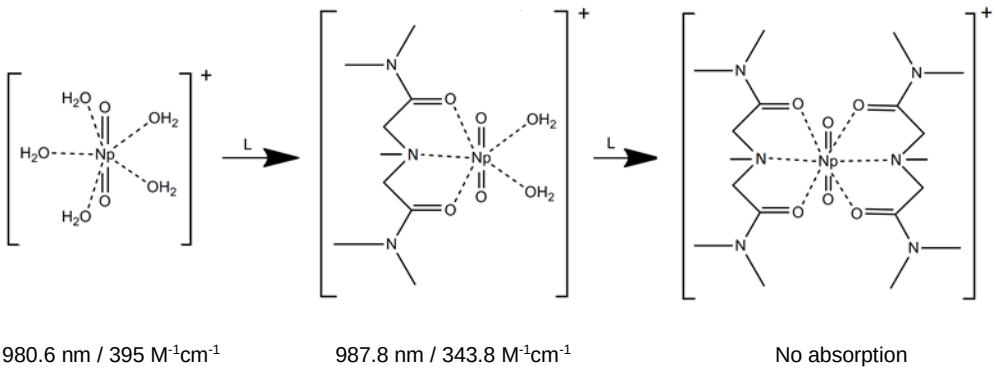

Figure 6. Stepwise formation of NpO_2^+/MABDMA complexes and their optical absorption properties (band position / molar absorptivity) from this work.

The free aquo NpO_2^+ ion and the 1:1 complex $NpO_2(L)^+$ show optical absorption bands at 980.6 nm and 987.8 nm, respectively, implying that neither of the two species is centrosymmetric. The free aquo NpO_2^+ ion is not centrosymmetric because there are five H_2O molecules in the equatorial plane as determined by X-ray absorption in this study (Table 2) and other studies.[41,42] The 1:1 complex, $NpO_2(L)^+$, is not centrosymmetric either, because its equatorial plane consists of one tridentate ligand and two water molecules as shown by EXAFS (section 3.4). As to the 1:2 complex, $NpO_2(L)_2^+$, the continuous decrease and gradual disappearance of the absorbance in Phase II of the spectrophotometric titration strongly imply that $NpO_2(L)_2^+$ does not absorb in the near IR region, and this implication is validated by the DFT calculation that indicates $NpO_2(L)_2^+$ is centrosymmetric.

4. Conclusion

NpO_2^+ forms moderately strong 1:1 and 1:2 complexes with three N-functionalized diacetamide ligands in aqueous solutions, $NpO_2(L)^+$ and $NpO_2(L)_2^+$. The complexation of NpO_2^+ with the imine nitrogen-linked diacetamides is stronger than that with analogous ether oxygen-linked diacetamide

ligand. By integrating the structural information from EXAFS and the theoretical calculation of the energetics, the complexation model that includes the formation of an optically absorbing $NpO_2(L)^+$ complex and an optically non-absorbing $NpO_2(L)_2^+$ complex is validated.

Acknowledgements

This work was supported by the Director, Office of Science, Office of Basic Energy Sciences under U.S. Department of Energy Contract No. DE-AC02-05CH11231 at Lawrence Berkeley National Laboratory (LBNL). The EXAFS experiments were carried out at Stanford Synchrotron Radiation Laboratory (SSRL), a user facility operated for the U.S. DOE by Stanford University. Y. Gao acknowledges financial support from the China Scholarship Council for her visit to LBNL. The computational work at University of Udine was supported by the "Piano Strategico d'Ateneo 2016-18".

ASSOCIATED CONTENT

Supporting Information. Experimental conditions of spectrophotometric titrations. This material is available free of charge via the Internet at http://pubs.acs.org.

AUTHOR INFORMATION

Corresponding Author

*Email: lxzhang@lbl.gov, (Tel) +1-510-486-5427; andrea.melchior@uniud.it, (Tel) +39 0432 558882.

References

(1) *Yucca Mountain Science and Engineering Report Rev. 1*; U. S. Department of Energy: North Las Vegas, 2002.

(2) Yang, Y.; Zhang, Z, Liu, G.; Luo, S.; Rao, L. Effect of Temperature on the Complexation of NpO_2^+ with Benzoic Acid: Spectrophotometric and Calorimetric Studies. *J. Chem. Thermodyn.* **2015**, *80*, 73-78.

(3) Zhang, Z; Yang, Y; Liu G; Luo, S: Rao, L. Effect of temperature on the thermodynamic and spectroscopic properties of Np(V) complexes with picolinate. *RSC Adv.*, **2015**, *5*, 75483-75490.

(4) Tian, G.; Rao, L.; Teat, S. J. Thermodynamics, Optical Properties, and Coordination Modes of Np(V) with Dipicolinic Acid. *Inorg. Chem.* **2009**, *48* (21), 10158–10164.

(5) Yang, Y.; Zhang, Z.; Luo, S.; Rao, L. Complexation of Np(V) Ions with 1,10-Phenanthroline-2,9-Dicarboxylic Acid: Spectrophotometric and Microcalorimetric Studies. *Eur. J. Inorg. Chem.* **2014**, *2014* (32), 5561–5566.

(6) Jensen, M. P.; Nash, K. L. Thermodynamics of dioxoneptunium(V) Complexation by Dicarboxylic Acids. *Radiochim. Acta* **2001**, *89* (9), 557–564.

(7) Rizkalla, E. N.; Nectoux, F.; Dabos-Seignon, S.; Pages, M. Complexation of Neptunium(V) by Halo- and Hydroxycarboxylate Ligands. *Radiochim. Acta* **1990**, *51* (3), 113–118.

(8) Eberle, S. H.; Wede, U. Chelatgleichgewichte Fünfwertiger Transurane Mit Aminopolykarbonsäuren. *J. Inorg. Nucl. Chem.* **1970**, *32* (1), 109–117.

(9) Tian, G.; Rao, L. Complexation of NpO_2^+ with N-Methyl-Iminodiacetic Acid: A Comparison with Iminodiacetic and Dipicolinic Acids. *Dalton Trans.* **2010**, *39* (41), 9866–9871.

(10) Ansari, S. A.; Bhattacharyya, A.; Zhang, Z.; Rao, L. Complexation of Neptunium(V) with Glutaroimide Dioxime: A Study by Absorption Spectroscopy, Microcalorimetry, and Density Functional Theory Calculations. *Inorg. Chem.* **2015**, *54* (17), 8693–8698.

(11) Ansari, S. A.; Pathak, P.; Mohapatra, P. K.; Manchanda, V. K. Chemistry of Diglycolamides: Promising Extractants for Actinide Partitioning. *Chem. Rev.* **2012**, *112* (3), 1751–1772.

(12) Tian, G. X.; Zhang, P.; Wang, J. C.; Rao, L. F. Extraction of actinide(III, IV, V, VI) Ions and TcO_4^- by N,N,N ',N '-Tetraisobutyl-3-Oxa-Glutaramide. *Solvent Extr. Ion Exch.* **2005**, *23* (5), 631–643.

(13) Tian, G.; Xu, J.; Rao, L. Optical Absorption and Structure of a Highly Symmetrical Neptunium(v) Diamide Complex. *Angew. Chemie - Int. Ed.* **2005**, *44* (38), 6200–6203.

(14) Dau, P. V.; Zhang, Z.; Dau, P. D.; Gibson, J. K.; Rao, L. Thermodynamic Study of the Complexation between Nd^{3+} and Functionalized Diacetamide Ligands in Solution. *Dalton Trans.* **2016**, *45* (30), 11968–11975.

(15) Dau, P. V.; Zhang, Z.; Gao, Y.; Parker, B. F.; Dau, P. D.; Gibson, J. K.; Arnold, J.; Tolazzi, M.; Melchior, A.; Rao, L. Thermodynamic, Structural, and Computational Investigation on the Complexation between UO_2^{2+} and Amine-Functionalized Diacetamide Ligands in Aqueous Solution. *Inorg. Chem.* **2018**, *57* (4), 2122–2131.

(16) Laporte, O.; Meggers, W. F. Some Rules of Spectral Structure. *J. Opt. Soc. Am.* **1925**, *11* (5), 459.

(17) Matsika, S.; Pitzer, R. M.; Reed, D. T. Intensities in the Spectra of Actinyl Ions. *J. Phys. Chem. A* **2000**, *104* (51), 11983–11992.

(18) Matsika, S.; Pitzer, R. M. Electronic Spectrum of the NpO_2^{2+} and NpO_2^{+} Ions. *J. Phys. Chem. A* **2000**, *104* (17), 4064–4068.

(19) Matsika, S.; Zhang, Z.; Brozell, S. R.; Blaudeau, J. P.; Wang, Q.; Pitzer, R. M. Electronic Structure and Spectra of Actinyl Ions. *J. Phys. Chem. A* **2001**, *105* (15), 3825–3828.

(20) Infante, I.; Gomes, A. S. P.; Visscher, L. On the Performance of the Intermediate Hamiltonian Fock-Space Coupled-Cluster Method on Linear Triatomic Molecules: The Electronic Spectra of NpO_2^{+}, NpO_2^{2+}, and PuO_2^{2+}. *J. Chem. Phys.* **2006**, *125* (7), 74301.

(21) Rao, L. F.; Srinivasan, T. G.; Garnov, A. Y.; Zanonato, P. L.; Di Bernardo, P.; Bismondo, A. Hydrolysis of neptunium(V) at Variable Temperatures (10-85 °C). *Geochim. Cosmochim. Acta* **2004**, *68* (23), 4821–4830.

(22) Gran, G. Determination of the Equivalence Point in Potentiometric Titrations. Part II. *Analyst* **1952**, *77* (920), 661.

(23) Gans, P.; Sabatini, A.; Vacca, A. Investigation of Equilibria in Solution. Determination of Equilibrium Constants with the HYPERQUAD Suite of Programs. *Talanta* **1996**, *43* (10), 1739–1753.

(24) Ravel, B.; Newville, M. *ATHENA* , *ARTEMIS* , *HEPHAESTUS* : Data Analysis for X-Ray Absorption Spectroscopy Using *IFEFFIT*. *J. Synchrotron Radiat.* **2005**, *12* (4), 537–541.

(25) Zabinsky, S. I.; Rehr, J. J.; Ankudinov, A.; Albers, R. C.; Eller, M. J. Multiple-Scattering Calculations of X-Ray-Absorption Spectra. *Phys. Rev. B* **1995**, *52* (4), 2995–3009.

(26) Becke, A. D. A New Mixing of Hartree-Fock and Local Density-Functional Theories. *J.Chem.Phys.* **1993**, *98* (2), 1372–1377.

(27) Lee, C. T.; Yang, W. T.; Parr, R. G. Development of the Colle-Salvetti Correlation-Energy Formula Into A Functional of the Electron-Density. *Phys.Rev.B* **1988**, *37* (2), 785–789.

(28) Di Bernardo, P.; Zanonato, P. L. P. L.; Benetollo, F.; Melchior, A.; Tolazzi, M.; Rao, L. Energetics and Structure of uranium(VI)-Acetate Complexes in Dimethyl Sulfoxide. *Inorg. Chem.* **2012**, *51* (16), 9045–9055.

(29) Endrizzi, F.; Melchior, A.; Tolazzi, M.; Rao, L. Complexation of uranium(VI) with Glutarimidoxioxime: Thermodynamic and Computational Studies. *Dalton Trans.* **2015**, *44* (31), 13835–13844.

(30) Grimme, S.; Antony, J.; Ehrlich, S.; Krieg, H. A Consistent and Accurate *Ab Initio*

Parametrization of Density Functional Dispersion Correction (DFT-D) for the 94 Elements H-Pu. *J. Chem. Phys.* **2010**, *132* (15), 154104.

(31) Jacobsen, H.; Cavallo, L. On the Accuracy of DFT Methods in Reproducing Ligand Substitution Energies for Transition Metal Complexes in Solution: The Role of Dispersive Interactions. *ChemPhysChem* **2012**, *13* (2), 562–569.

(32) Kuchle, W.; Dolg, M.; Stoll, H.; Preuss, H. Energy-Adjusted Pseudopotentials for the Actinides - Parameter Sets and Test Calculations for Thorium and Thorium Monoxide. *J.Chem.Phys.* **1994**, *100* (10), 7535–7542.

(33) Tomasi, J.; Mennucci, B.; Cammi, R. Quantum Mechanical Continuum Solvation Models. *Chem. Rev.* **2005**, *105* (8), 2999–3093.

(34) Gaussian 16, Revision A.03, Frisch, M. J.; Trucks, G. W.; Schlegel, H. B.; Scuseria, G. E.; Robb, M. A.; Cheeseman, J. R.; Scalmani, G.; Barone, V.; Petersson, G. A.; Nakatsuji, H.; Li, X.; Caricato, M.; Marenich, A. V.; Bloino, J.; Janesko, B. G.; Gomperts, R.; Mennucci, B.; Hratchian, H. P.; Ortiz, J. V.; Izmaylov, A. F.; Sonnenberg, J. L.; Williams-Young, D.; Ding, F.; Lipparini, F.; Egidi, F.; Goings, J.; Peng, B.; Petrone, A.; Henderson, T.; Ranasinghe, D.; Zakrzewski, V. G.; Gao, J.; Rega, N.; Zheng, G.; Liang, W.; Hada, M.; Ehara, M.; Toyota, K.; Fukuda, R.; Hasegawa, J.; Ishida, M.; Nakajima, T.; Honda, Y.; Kitao, O.; Nakai, H.; Vreven, T.; Throssell, K.; Montgomery, J. A., Jr.; Peralta, J. E.; Ogliaro, F.; Bearpark, M. J.; Heyd, J. J.; Brothers, E. N.; Kudin, K. N.; Staroverov, V. N.; Keith, T. A.; Kobayashi, R.; Normand, J.; Raghavachari, K.; Rendell, A. P.; Burant, J. C.; Iyengar, S. S.; Tomasi, J.; Cossi, M.; Millam, J. M.; Klene, M.; Adamo, C.; Cammi, R.; Ochterski, J. W.; Martin, R. L.; Morokuma, K.; Farkas, O.; Foresman, J. B.; Fox, D. J. Gaussian, Inc., Wallingford CT, 2016.

(35) Tian, G.; Rao, L. Complexation of Np(V) with Oxalate at 283–343 K: Spectroscopic and Microcalorimetric Studies. *Dalt. Trans.* **2012**, *41* (2), 448–452.

(36) Tian, G.; Rao, L.; Xia, Y.; Friese, J. I. Complexation of Neptunium(V) with Fluoride at Elevated Temperatures, *J. Therm. Anal.Calorim.*, **2009**, *95* (2), 415-419.

(37) Rao, L.; Tian, G.; Xia, Y.; Friese, J. I. Spectrophotometric and Calorimetric Studies of Np(V) Complexation with Sulfate at 10-70^{o}C, *J. Therm. Anal.Calorim.*, **2009**, *95* (2), 409-413.

(38) Rao, L.; Tian, G. Symmetry, Optical Properties and Thermodynamics of neptunium(V) Complexes. *Symmetry*, **2010**, 2(1), 1–14.

(39) Tian, G.; Rao, L.; Oliver, A. Symmetry and Optical Spectra: a "silent" 1:2 Np(V)-Oxydiacetate Complex. *Chem. Commun.* **2007**, *2* (40), 4119–4121.

(40) Smith, R. M.; Martell, A. E. Critical Stability Constant Database 46. National Institute of Science and Technology (NIST): Gaithersburg, MD 2003.

(41) Jean-Marie, C.; Chlsholm-Brause, C. J.; Brown, G. E.; Parks, G. A.; Conradson, S. D.; Gary Eller, P.; Trlay, I. R.; Hobart, D. E.; Arend, M. EXAFS Spectroscopic Study of Neptunium(V) Sorption at the α-FeOOH/Water Interface. *Environ. Sci. Technol.* **1992**, *26* (2), 376–382.

(42) Allen, P. G.; Bucher, J. J.; Shuh, D. K.; Edelstein, N. M.; Reich, T. Investigation of Aquo and Chloro Complexes of UO_2^{2+}, NpO_2^{+}, Np^{4+}, and Pu^{3+} by X-Ray Absorption Fine Structure Spectroscopy. *Inorg. Chem.* **1997**, *36* (21), 4676–4683.

(43) Bessonov, A. A.; Afonas'eva, T. V.; Krot, N. N. Electronic Absorption Spectra of Solid Compounds of Actinoids. IV. Perchlorate, Chloride and Nitrate of neptunium(V). *Radiokhimya* **1991**, *33* (3), 47–52.

(44) Grigor'ev, M. S.; Baturin, N. A.; Bessonov, A. A.; Krot, N. N. Crystal Structure and Electronic Absorption Spectrum of neptunyl(V) Perchlorate $NpO_2ClO_4 \cdot 4H_2O$. *Radiokhimya* **1995**, *37* (1), 15–18.

TOC Graphic

NpO_2^{+} forms moderately strong NpO_2L^{+} and $NpO_2(L)_2^{+}$ complexes with amine-functionalized diacetamides and the $NpO_2(L)_2^{+}$ complexes are "silent" in near-IR optical absorption.

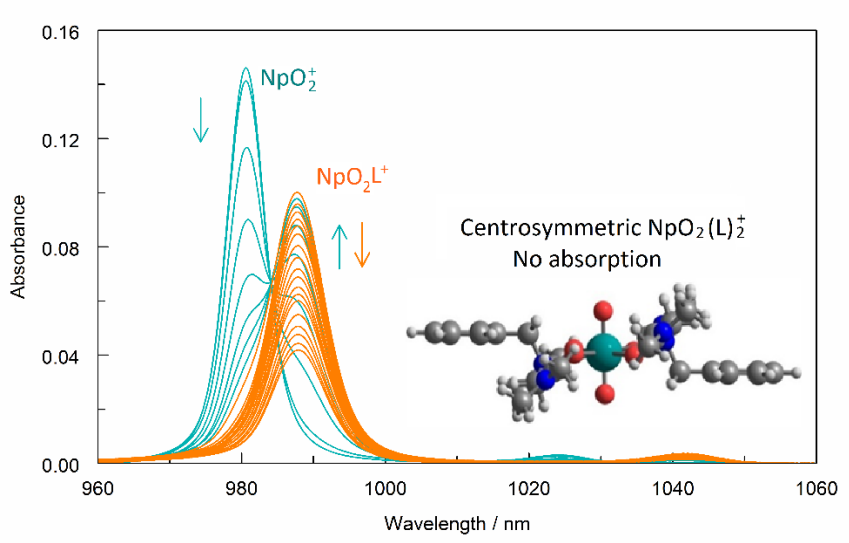

Supporting Information

Table S1 Experimental conditions for spectrophotometric titrations to determine the stability constants of NpO_2^{+} complexes with BnABDMA, ABDMA, and MABDMA. The initial volume in the cuvette was 2.10 ml, and a total of 1.08-1.15 mL of titrant was added in each titration.

Ligand	Titration #	Initial Conditions, mM			Titrant, mM		
		C_{Np}	C_H	$C_{Nitrate}$	C_L	C_H	$C_{Nitrate}$
BnABDMA	1	0.362	0.419	1000	157	0	1000
	2	0.290	0.338	1000	157	0	1000

ABDMA	1	0.390	0.448	1000	53.44	4.79	1000
	2	0.328	0.381	1000	53.44	4.79	1000
MABDMA	1	0.386	0.443	1000	38.0	0	1000
	2	0.310	0.357	1000	38.0	0	1000

Table S2 Selected bond distances (Å) in the DFT minimum energy structures of the $NpO_2L_2^+$ complexes calculated in PCM water (Figure 5) For comparison also data for $[NpO_2(H_2O)_5]^+$ are reported. In the last column the energy difference ΔG (kJ mol^{-1}) relative to the most stable isomer is reported.

		$Np\text{-}O_{ax}$	$Np\text{-}O_{eq}$	Np-N	ΔG_{water}
$Np(H_2O)_5^+$		1.793	2.551	-	-
$Np(ABDMA)_2^+$	A	1.823	2.578	2.742	0.0
	B	1.820	2.578	2.741	8.2
	C	1.824	2.577	2.762	8.4
$Np(MABDMA)_2^+$	D	1.821	2.570	2.799	0.0
	E	1.818	2.552	2.841	10.5
	F	1.824	2.570	2.806	5.2
$Np(BnABDMA)_2^+$	G	1.818	2.567	2.803	0.0
	H	1.817	2.580	2.861	31.5
	I	1.823	2.576	2.796	22.2